점성을 가진 음질이 입혀진 원형평판으로부터의 음악복사

A Study on the Sound Radiation from a Clamped Circular Plate with Viscoelastic layer by Impact Force

*전 재 진(Jeon, J. J.)
**이 병 호(Lee, B. H.)

요 약

본 논문에서는 충격으로 인한 점탄성층을 가진 경계가 고정된 원형 평판으로부터의 음압복사에 대해 이론적, 실험적으로 연구한다. 층을 가진 평판의 운동을 모우드 해석법과 회전 관성효과와 전단력에 의한 변형을 고려한 Mindlin 의 평판이론으로부터 구한 고유치를 이용하여 구한다. 탄성구와 평판사이의 접촉력은 Hertz 이론으로 구하고 평판의 진동으로부터 복사되는 음압은 Rayleigh integral 에 의해 구한다. 또한 층을 가진 평판으로부터 복사되는 음의 파형과 발생되는 음을 감소시키는 방법을 예측한다.

ABSTRACT

In this paper, the sound radiation from a clamped circular plate with a viscoelastic layer excited by impact force is studied both analytically and experimentally. The composite plate vibrations are obtained by using the normal mode analysis and the eigenvalues are obtained by a Mindlin plate theory including

*Dept. of Mech. Eng. KAIST 박사과정
**Dept. of Mech. Eng. KAIST 교수.

the rotary inertia and shear def..... ped between the ball and the plate with attached layers is obtained by Hertz contact theory. The radiated sound pressure is calculated by the Rayleigh integral. Prediction of the waveforms of sound radiating from the plate with attached layers and a method for reducing noise generation from the plate by impact force are also shown in this paper.

INTRODUCTION

Sound radiation from mechanical systems results mainly from the vibration by various kinds of the external forces. The mechanism of the sound radiation depends on the geometry and the nature of contact between the impinging objects.[1]

Many investigations on impulsive vibration and sound radiation have been performed. Strasberg[2] calculated the radiated acoustic power from a periodically struct diaphragm in frequency domain. The formulation of the sound radiation was based on the results of Lax.[3] He investigated the radiation on a circular clamped plate using the Rayleigh integral equation. Akay et al.[4,5] investigated impact of a ball on a clamped circular plate. Takahagi et al.[6] evaluated the waveform of the impulsive sound pressure from the plates of various thicknesses, taking into account of the effects of rotary inertia and shear deformation.

The above investigations are all limited to the sound radiation from only a simple plate. However, recently, many papers have been investigated to the dynamic response of composite plates consisting of one or two outer layers because of their increasing application in various fields. Venkatesan et al.[7] investigated free vibrational characteristics of layered plates including the shear deformation and rotatory inertia effect. Krzysztof Poltorak et al.[8] dealt with a method for solving free vibration problems of three-layered isotropic plates of arbitrary shape with a clamped edge. However, they have not discussed about the sound radiation from the composite plate.

In this paper, the transient sound radiation from a composite, clamped circular plate with viscoelastic layer is studied both analytically and experimentally. The layered plate vibrations are obtained by using the mode analysis and the eigenvalues are obtained by a Mindlin plate theory. The contact force developed during the impact of a ball with composite plate is obtained by the Hertz theory. The radiated sound pressure is calculated by the Rayleigh integral. Also we suggest a method for reducing the sound radiation.

I. THEORETICAL ANALYSIS

A. Axisymmetric vibration equation including effects of rotary inertia and shear

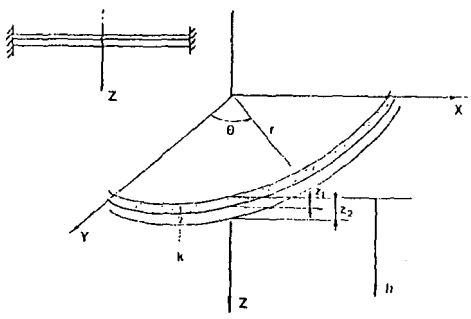

Fig. 1 Layered plate in cylindrical coordinates.

The equation of axisymmetric motion for the displacement of the clamped circular plate consisting of multilayer, as shown in Fig.1, are derived from Mindlin's theory which includes effects of the rotary inertia and the shear deformation. We can write the equation of motion of the layered plate as

$$\nabla^4 w(r,\theta,t)-\frac{R_0}{k}\nabla^2\ddot{w}(r,\theta,t)+\frac{R_0 A}{CA-B^2}\times\ddot{w}(r,\theta,t)=F(r,\theta,t) \quad (1)$$

Where

$$R_0=\sum_{m=1}^{n}\int_{h_{m-1}}^{h_m}\rho^m dz$$

$$h_0=\sum_{m=1}^{n}\int_{h_{m-1}}^{h_m}\rho^m z\,dz/R_0$$

$$(A,B,C)=\sum_{m=1}^{n}\int_{h_{m-1}-h_0}^{h_m-h_0}Q^m(1,z,z^2)dz$$

$$Q^m=E_m/(1-\nu_m^2),\quad D=\frac{CA-B^2}{A}$$

$$K=\sum_{m=1}^{n}\int_{h_{m-1}}^{h_m-h_0}-h_0\,\kappa_s\frac{E_m}{2(1+\nu_m)}dz$$

where sub- and superscript m denote the m-th layer and ρ^m is the density, ν_m the Poisson's ratio, and Em the Young's modulus of the m-th layer. $\kappa_s=\pi^2/12$ is a numerical factor depending on the shape of the cross section and in the case of plate

The general solution of the eigenvalue problem of the Eq.(1) is given by

$$W(r)=G_1 J_0(\mu_1 r)+G_2 I_0(\mu_2 r) \quad (3)$$

where

$$\mu_1^2=\frac{C_1+\sqrt{C_1^2-4C_2}}{2}\qquad \mu_2^2=\frac{-C_1+\sqrt{C_1^2-4C_2}}{2} \quad (4)$$

where

$$C_1=\frac{R_0\omega^2}{K}\qquad C_2=-\frac{A\omega^2 R_0}{DA-B^2}$$

We can obtain the frequency equation from the boundary condition, $\frac{\partial w}{\partial r}=0$ at r=0.

$$\mu_1 J_1(\mu_1 a)\,I_0(\mu_2 a)+\mu_2 J_0(\mu_1 a)\,I_1(\mu_2 a)=0 \quad (5)$$

for the axisymmetric layered circular plate of radius a, the normal mode shapes are given by

$$W_n(r)=G\left(J_0(\mu_1 r)-\frac{J_0(\mu_1 a)}{I_0(\mu_2 a)}I_0(\mu_2 r)\right) \quad (6)$$

where G is obtained from the normalization.

$$G=\frac{1}{\sqrt{\rho h\pi a^2}}\left[2J_0^2(\mu_1 a)+\left(1-\frac{\mu_1^2}{\mu_2^2}\right)J_1^2(\mu_1 a)\right]^{-\frac{1}{2}}$$

B. Impact force

The representation for the contact force developed during elastic impact of a ball of radius R with semi-infinite viscoelastic plate was given by Phillips et al.[9] and W. Goldsmith[10] as a function of the relative displacement of impinging ball and the impacted plane surface. In the case that the duration of contact is shorter than the duration which the flexural waves are reflected back from boundary to the center of plate, we can apply the contact force for the semi-infinite viscoelastic plate to this paper.

$$F(t)=k\alpha(t)^{3/2} \quad (7)$$

where

$$k=\frac{4}{3}\sqrt{R}\left(\frac{1-\nu_1^2}{E_1}+\frac{1-\nu^{*2}}{E^*}\right)^{-1} \qquad (7-1)$$

where ν_1, ν^* and E_1, E^* are Poisson's ratios and elasticity moduli of the ball and the plate, respectively.

The contact force representation in Eq.(7) is an extension of the well-known Hertz contact theory. In the case of the sphere impinging the plate, the time history of the contact force obtained from the following equation.

$$\frac{d^2}{dt^2}\alpha(t)+\left[\frac{k}{m}+\Gamma k\frac{d}{dt}\right]\alpha(t)^{3/2}=0 \qquad (8)$$

where

$$\Gamma=\frac{1}{8}\left[\frac{1}{\rho hD}\right]^{1/2}, \quad \rho=\frac{1}{h}\sum\rho_k(z_k-z_{k-1})$$

and m is the mass of the striker. Eq.(8) is non-dimensionalized to

$$\frac{d^2}{d\tau^2}\bar{\alpha}(t)+\left[1+\bar{\lambda}\frac{d}{d\tau}\right]\bar{\alpha}(t)^{3/2}=0 \qquad (8-1)$$

where $\tau=t/T$, $\bar{\alpha}=\alpha/TV$, and $T=0.311T_H$. T_H is the duration of contact predicted by Hertz theory for semi-infinite solid and V is the impinging velocity. Inelasticity parameter is given by $\bar{\lambda}=m/(0.311T_H Z)$, where m is the mass of the striker and $Z=8(\rho hD)^{1/2}$ is the impedance of the plate at the impact point.

The force time history obtained from Eq.(8) is plotted for various impinging velocities and thicknesses of plate in Figs.2 and 3 and is plotted for various thicknesses of attached layer in Fig.4. As the thickness of plate increases the contact time history resembles a half-period sine wave. Inelasticity parameter is zero for the infinite rigid surface. In this paper the impact force is represented as

$$F(r_j, t)=F_0\, e^{-\lambda\frac{\pi}{d}t}\sin\frac{\pi}{d}t\,\frac{\delta(r-r_j)}{2\pi r}$$

$$0\leqq t\leqq d \qquad (9)$$

where the duration of contact d is obtained from Eq.(8), F_0 the magnitude of contact force and r_j a point that the impact force acts. The para-

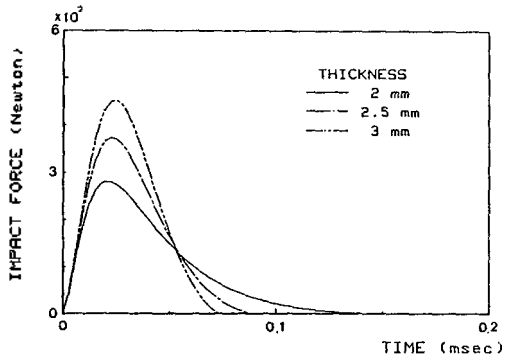

Fig. 2 Impact force time history for various thicknesses. Impacting velocity v=1 m/sec and steel ball of 1.504 cm diameter and steel plate of 28 cm diameter.

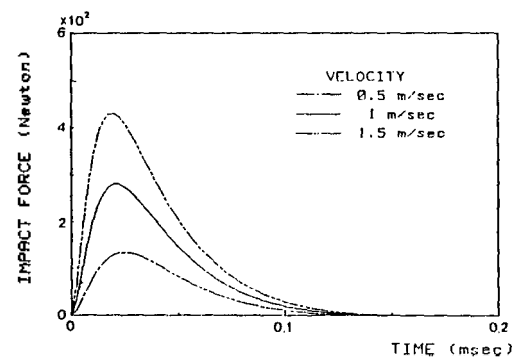

Fig. 3 Impact force time history for various impacting velocities. Bare steel plate of 2 mm thickness and steel ball of 1.504 cm diameter.

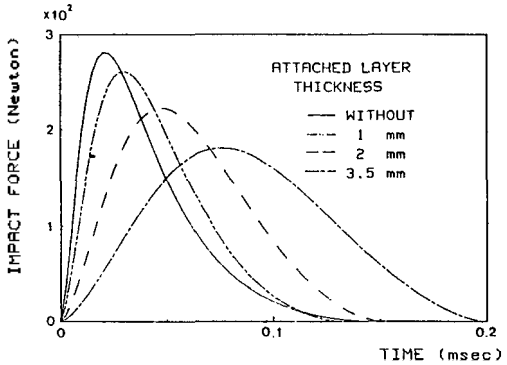

Fig. 4 Impact force time history for various attached layer thicknesses. Impacting velocity v=1 m/sec, steel ball of 1.504 cm diameter and bare steel plate of 2 mm thickness. Layer material is rubber.

meter λ is closely connected with the inelasticity.

C. Vibration response of the plate

As using the normal mode method, Laplace transform and convolution integral, the displacement response of a circular plate, initially undeformed and at rest, to the impact force given in Eq.(9) can be written as

$$W(r,\theta,t)=F_0\sum_{m,n=0}^{\infty}\frac{W_{mn}(r_f,\theta_f)\,W_{mn}(r,\theta)}{\omega_{mn}(1+j\eta)^{1/2}}\int_0^t e^{-\lambda\frac{\pi}{d}\tau}\sin\frac{\pi}{d}\tau\, e^{-\frac{\eta}{2}\omega_{mn}t} \quad (10)$$

$$*\sin[\omega^*_{mn}(t-\tau)]\,[H(\tau)-H(\tau-a)]\,d\tau$$

where ω_{mn} are the natural frequencies of the plate, Wmn are the normal mode function of the plates, (r_f, θ_f) the position of the impact force F(t) and H(t) is a unit step Heaviside function.

In the case of the axisymmetric vibration, m=0 and the mode shapes do not depend upon θ.

The displacement response of a clamped circular plate to an impact force can be written as

i) $t \leqq d$

$$W(r,\theta,t)=F_0\sum_{m,n=1}^{\infty}\frac{W_{mn}(r_f,\theta_f)\,W_{mn}(r,\theta)}{2\omega^*_{mn}}\left[\frac{1}{|(\omega_0-\omega^*_{mn})^2+(\frac{\eta}{2}\omega_{mn}-\lambda\omega_0)^2|^{1/2}}\times\right.$$

$$\times|e^{-\frac{\eta}{2}\omega_{mn}t}\sin(\omega^*_{mn}t+\Psi_1)-e^{-\lambda\omega_0 t}\sin(\omega_0 t+\Psi_1)|$$

$$+\frac{1}{|(\omega_0+\omega^*_{mn})^2+(\frac{\eta}{2}\omega_{mn}-\lambda\omega_0)^2|^{1/2}}$$

$$\left.|e^{-\lambda\omega_0 t}\sin(\omega_0 t+\Psi_2)+e^{-\frac{\eta}{2}\omega_{mn}t}\sin(\omega^*_{mn}t-\Psi_2)|\right] \quad (11-1)$$

ii) $t>d$

$$W(r,\theta,t)=F_0\sum_{m,n=0}^{\infty}\frac{W_{mn}(r_f,\theta_f)\,W_{mn}(r,\theta)}{2\omega^*_{mn}}\left[\frac{1}{|(\omega_0-\omega^*_{mn})^2+(\frac{\eta}{2}\omega_{mn}-\lambda\omega_0)^2|^{1/2}}\right.$$

$$\times|e^{-\frac{\eta}{2}\omega_{mn}t}\sin(\omega^*_{mn}t+\Psi_1)-e^{-\frac{\eta}{2}\omega_{mn}(t-d)-\lambda\omega_0 d}\sin(\omega_0 d+\omega^*_{mn}(t-d)+\Psi_1)|$$

$$+\frac{1}{|(\omega_0+\omega^*_{mn})+(\frac{\eta}{2}\omega_{mn}-\lambda\omega_0)^2|^{1/2}}|e^{-\frac{\eta}{2}\omega_{mn}t}\sin(\omega^*_{mn}t-\Psi_2)+e^{-\frac{\eta}{2}\omega_{mn}(t-d)-\lambda\omega_0 d}$$

$$\left.\sin(\omega_0 d-\omega^*_{mn}(t-d)+\Psi_2)|\right]$$

where

$$\omega_0=\pi/d$$

$$\omega^*_{mn} = \sqrt{1 - \frac{\eta^2}{2}}\,\omega_{mn}$$

$$\Psi_1 = \tan^{-1}\frac{\frac{\eta}{2}\omega_{mn} - \lambda\omega_o}{\omega_o - \omega^*_{mn}}$$

$$\Psi_2 = \tan^{-1}\frac{\frac{\eta}{2}\omega_{mn} - \lambda\omega_o}{\omega_o + \omega^*_{mn}}$$

and η is a loss factor.

The velocity and acceleration of the plate are obtained by differentiation of the Eq.(11), once and twice, respectively.

The loss factor η of the plate with attached layer is obtained from the complex transformed flexural rigidity. For many cases, the structural damping is almost the same as the material damping and therefore the loss factor can be assumed to be zero. However, for structures which the joint damping is high, the structural damping could be an important factor. If the damping layers have a high loss factor, $c\frac{\partial w}{\partial t}$ term is involved to Eqs.(1), where c is a damping coefficient.

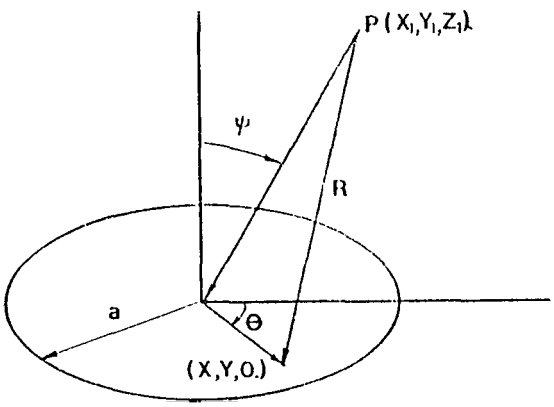

Fig. 5 Coordinates related to the sound radiation from the circular plate.

II. SOUND RADIATION FROM THE TRANSIENT VIBRATING CIRCULAR PLATE

The sound pressure radiated from a vibrating plate is calculated by using the Rayleigh integral, the elements of the plate are regarded as the simple point source of an outgoing wave and they have a time delay. The acoustic pressure from a vibrating circular plate shown in Fig.5 is calculated as the following equation.[11,12]

$$P(R,\theta,\Psi,t) = \frac{\rho_o}{2\pi}\frac{\cos\Psi}{\cos\Psi+\beta}\iint \dot{W}\left(r,\theta,t-\frac{R}{C}\right)\frac{ds}{R} \quad (12)$$

where

$$R = [(x-x_1)^2 + (y-y_1)^2 + z_1^2]^{1/2}$$

$$r = (x^2+y^2)^{1/2}$$

where β is an acoustic admitance $\rho_o c/z(\omega)$ where $z(\omega)$ is a surface impedance and $\rho_o c$ a characteristic impedance of the ambient medium. $\dot{W}(r,\theta,t-R/C)$ is the acceleration-time response of the plate. From Eq.(11), the acceleration is given as

i) $t<d$, $t_1 = t - \frac{R}{C}$, $\zeta = \frac{\eta}{2}$

$$\dot{W}\left(r,\theta,t-\frac{R}{C}\right) = F_o\sum_{m=1,n=0}^{\infty}\frac{W_{mn}(r_1,\theta_1)\,W_{mn}(r,\theta)}{2\omega^*_{mn}}$$

$$\left[\frac{1}{(\omega_o-\omega^*_{mn})^2+(\zeta\omega_{mn}-\lambda\omega_o)^2}\right.$$

$$\times\{(\omega_o-\omega_{mn})\{(\zeta^2\omega^{*2}_{mn}+\omega^{*2}_{mn})\,e^{-\zeta\omega_{mn}t_1}\sin(\omega^*_{mn}t_1-\Psi_1)$$

$$+(1+\lambda^2)\omega_o^2\,e^{-\lambda\omega_o t_1}\sin(\omega_o t_1+\Psi_2)$$

$$+(\zeta\omega_{mn}-\lambda\omega_o)\times$$

$$\times\{(\zeta^2\omega_{mn}^2+\omega_{mn}^{*2})\,e^{-\zeta\omega_{mn}t_1}\cos(\omega_{mn}^{*}t_1-\Psi_1)$$

$$+(1+\lambda^2)\,\omega_o^2\,e^{-\lambda\omega_o t_1}\times$$

$$\times\cos(\omega_o t_1+\Psi_2)+\frac{1}{(\omega_o+\omega_{mn}^{*})^2+(\zeta\omega_{mn}-\lambda\omega_o)^2}$$

$$\{(\omega_o+\omega_{mn}^{*})\times$$

$$\times\{(1+\lambda^2)\,\omega_o^2\,e^{-\lambda\omega_o t_1}\sin(\omega_o t_2-\Psi_2)$$

$$+(\zeta^2\omega_{mn}^2+\omega_{mn}^{*2})\,e^{-\zeta\omega_{mn}t_2}\sin(\omega_{mn}^{*}t_1-\Psi_1)$$

$$+(\zeta\omega_{mn}-\lambda\omega_o)\}\{(1+\lambda^2)\,\omega_o^2\,e^{-\lambda\omega_o t_1}$$

$$\cos(\omega_o t_2-\Psi_2)-(\zeta^2\omega_{mn}^2+\omega_{mn}^{*2})\times$$

$$\times e^{-\zeta\omega_{mn}t_1}\cos(\omega_{mn}^{*}t_1-\Psi_1)\}\}\}$$

ii) $t>d$ $t_2=t-d-\dfrac{R}{C}$, $C_1=\zeta\omega_{mn}t_2+\lambda\omega_o d$

$$\dot{W}(r,\theta,t-\frac{R}{C})=F_o\sum_{m,n=0}^{\infty}\frac{W_{mn}(r_j,\theta_j)W_{mn}(r,\theta)}{2\omega_{mn}^{*}}$$

$$\left[\frac{1}{(\omega_o-\omega_{mn}^{*})^2+(\zeta\omega_{mn}-\lambda\omega_o)^2}\times\right.$$

$$\times\{(\omega_o-\omega_{mn}^{*})\{(\zeta^2\omega_{mn}^2+\omega_{mn}^{*2})\}\,e^{-\zeta\omega_{mn}t_1}$$

$$\sin(\omega_{mn}^{*}t_1-\Psi_1)-e^{-C_1}\sin(\omega_o d+\omega_{mn}^{2}t_2-\Psi_1)\}\}$$

$$+(\zeta\omega_{mn}-\lambda\omega_o)\{(\zeta^2\omega_{mn}^2+\omega_{mn}^{*2})\}\,e^{-\zeta\omega_{mn}t_1}$$

$$\cos(\omega_{mn}^{*}t_1-\Psi_1)-e^{-C_1}\cos(\omega_o d+\omega_{mn}^{*}t_2-\Psi_1)\}\}\}$$

$$\left.+\frac{1}{(\omega_o+\omega_{mn}^{*})^2+(\zeta\omega_{mn}-\lambda\omega_o)^2}\{(\omega_o+\omega_{mn}^{*})\right.$$

$$\{(\zeta^2\omega_{mn}^2+\omega_{mn}^{*2})\}\,e-\zeta\omega_{mn}t_1\sin(\omega_{mn}^{*}t_1-\Psi_1)+$$

$$+e^{-C_1}\sin(\omega_o d-\omega_{mn}^{*}t_2+\Psi_1)\}+(\zeta\omega_{mn}-\lambda\omega_o)$$

$$\{(\zeta^2\omega_{mn}^2+\omega_{mn}^{*2})\}\,e^{-C_1}\cos(\omega_o d-\omega_{mn}^{*}t_2+\Psi_1)$$

$$\left.-e^{-\zeta\omega_{mn}t_1}\cos(\omega_{mn}^{*}t_1-\Psi_1)\}\}\right]$$

where

$$\Psi_1=\tan^{-1}\frac{2\zeta\omega_{mn}\omega_{mn}^{*}}{\zeta^2\omega_{mn}^2-\omega_{mn}^{*2}}$$

$$\Psi_2=\tan^{-1}\frac{2\lambda}{1-\lambda^2}$$

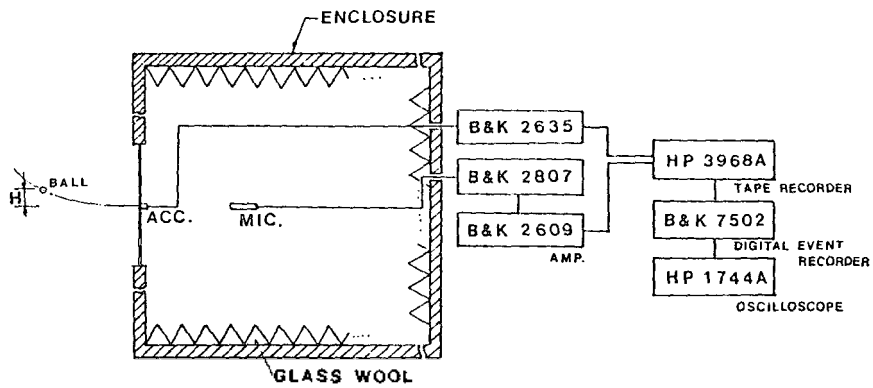

Fig. 6 Schematic diagram of the experiment.

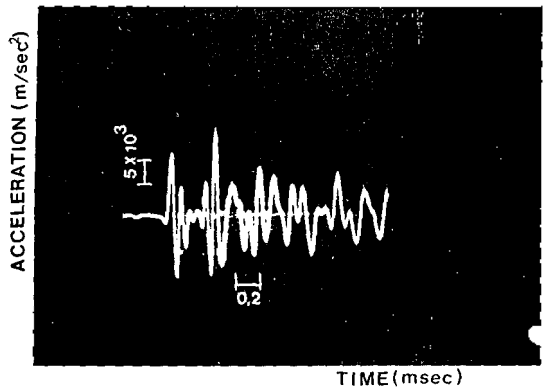

(a)

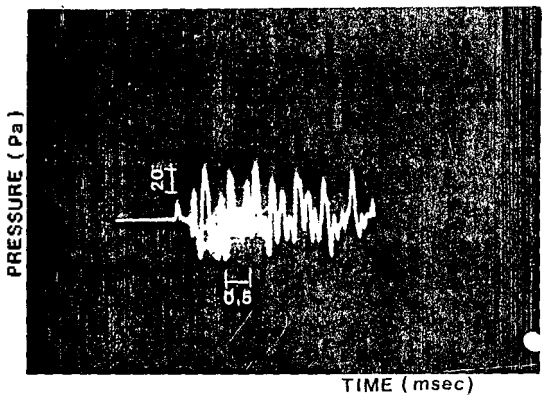

(b)

Fig. 7. Measured sound pressure waveform and acceleration response of the bare steel plate. Steel ball of 1.504 cm diameter and steel plate of 2 mm thickness and H=0.052 m. The position of microphone is 10 cm on z-axis.

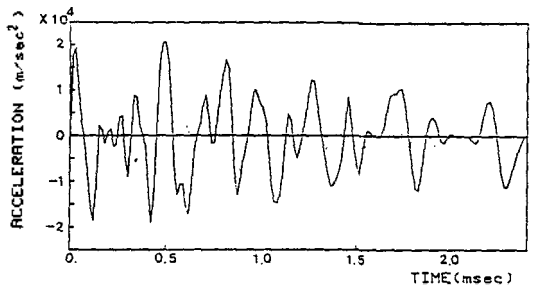

Fig. 8 Calculated acceleration waveform at impact point. Steel ball of 1.504 cm diameter, steel plate of 2 mm thickness and H=0.052 m.

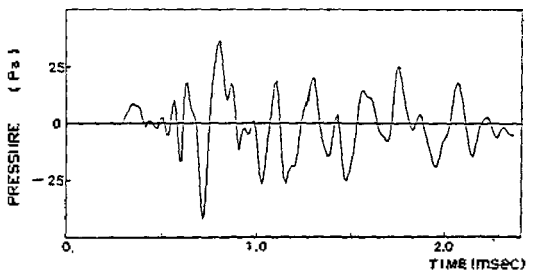

Fig. 9 Calculated sound pressure wave form on the axis of symmetry. Steel ball of 1.504 cm diameter, steel plate of 2 mm thickness and H= 0.052 m. The position of microphone is 10 cm on z-axis.

The waveform of the radiated sound pressure is obtained from Eqs.(12) and (13), and is plotted in Fig.9 for the case of bare steel plate by the impact force, and Fig.12 is plotted for that of the plate with attached layer.

III. EXPERIMENT

The experimental apparatus is shown in Fig.6. The circular plate was clamped with a rigid sandwich circular ring bolted together in order to fix rigidly the plate. The pressure waveforms were measured by a microphone(B&K 4134 1/2 inch diameter) in an anechoic enclosure as shown in Fig.6 and the acceleration in time domain was measured by accelerometer (B&K 4375).

Measurements were carried out to obtain the plate vibration response and the radiated sound

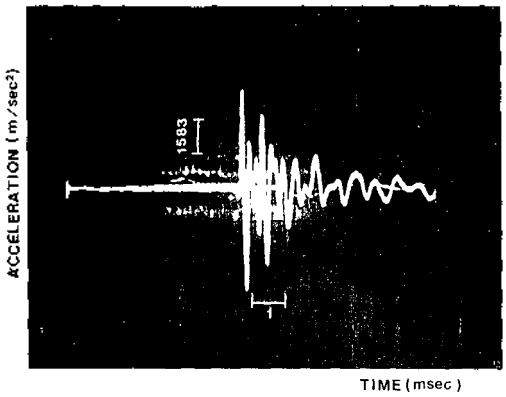

(a)

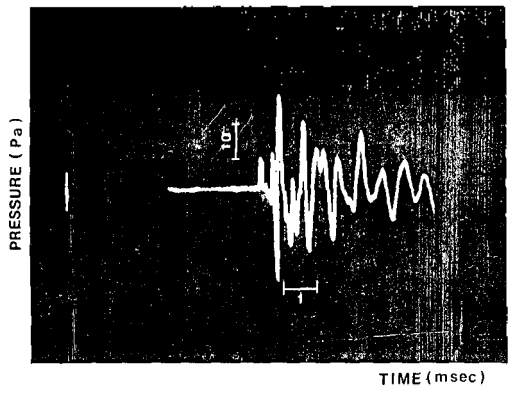

(b)

Fig.10 Measured acceleration response of the plate and the waveform of radiated sound pressure for Figs.9 and 10. The thickness of attached layer (rubber) is 3.5 mm, the diameter of steel ball 1.504 cm, the thickness of bare steel plate 2 mm and H=0.052 m. Impacting side: steel. The position of microphone is 10 cm on z-axis.

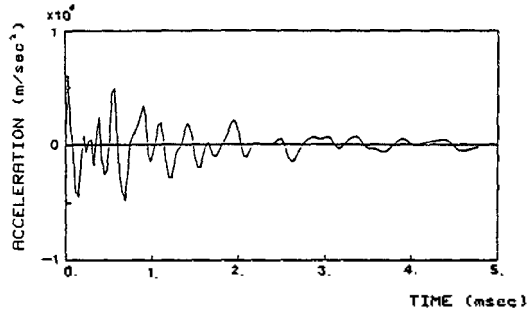

Fig.11 Calculated acceleration at impact point of the plate with attached layer for Fig.11(a). The thickness of layer is 3.5 mm-rubber, the diameter of steel ball 1.504 cm and H=0.052 m.

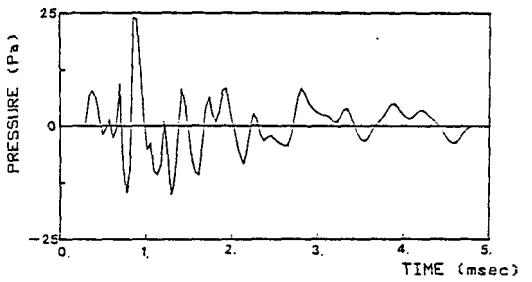

Fig.12 Calculated the waveform of the radiated sound from the plate with attached layer on the axis of symmetry for Fig.11(b). The thickness of layer is 3.5 mm-rubber, H=0.052 m and the diameter of steel ball 1.504 cm. The position of microphone is 10 cm on z-axis.

pressure waveforms for various circular plates with or without rubber coating. The bare and coated steel plate of 0.28 m-diameter were clamped at the edges and the plate stood vertical to the ground. The steel ball was dropped from a height H. The measured waveforms of the sound pressure and the acceleration are given in Figs.7. Analytical results corresponding to the experimental results, Fig.7, are shown in Figs.8 and 9. And the waveforms of the measured and calculated sound pressure and acceleration for the layered plate are shown in Figs.10-12.

IV. RESULTS AND DISCUSSIONS

The vibration and acoustic response of the clamped circular plate by an impact has been obtained analytically and experimentally. In the computation, the results have been taken the first 15 modes of the plate.

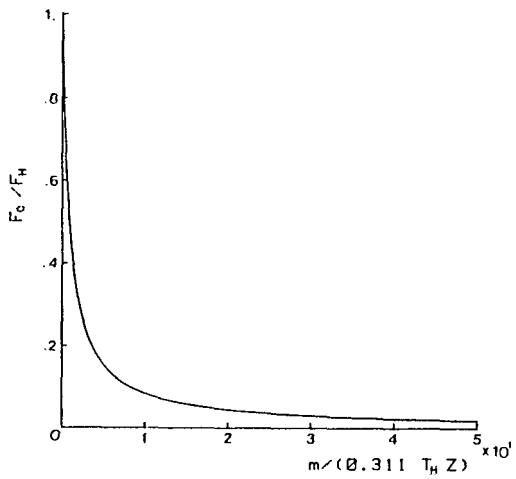

Fig.13 The amplitude of impact force as a function of plate inelasticity.

In this paper, we coat the viscoelastic material on the steel plate in order to reduce the noise and vibration. We find that the contact forces reduce as increasing the coating thickness and the duration is longer than the case of bare steel plate. From Figs.2,4 and Eq.(8-1), the dependence of the magnitude of the impact force, F_o, for the plate with viscoelastic layer on the inelasticity parameter λ and impedance Z_i of the plate can be approximated from the fig.13.

$$F_o = \frac{F_H}{1+1.1\lambda}\left(\frac{Z_b}{Z}\right)^3 \qquad (14)$$

where F_H is the Hertz contact force developed during elastic impact of a spherical striker with a rigid plane surface of a semi-infinite solid and λ is inelasticity parameter. From Fig.13, the contact force on the bare steel plate can be approximated as $F_H/(1+1.1\lambda)$. Z_b is the impedance of the bare steel plate. As the inelasticity parameter decreases, the waveforms of contact force become a half-sine shape.

The sound pessure- and acceleration-time histories is similar both in the analytical and experimental results, respectively. The first peak in the waveform of sound pressure and plate acceleration are due to the forced deformation of the plate. In Figs. 7-12, the theoretical and experimental results are shown that, immediately after the first peak of the sound pressure, there is no sound radiation until the flexural waves are reflected back from boundary to the center of plate.

After the reflected flexural waves reach at the area of impact, the plate becomes the state of damped free vibrations, and the vibrations have an effect on the ringing radiation from plate. The lack of sound radiation due to the flexural waves before the state of damped free vibration can be explained by considering the sound radiation mechanism from the flexural waves in the finite plates. Below the critical frequency the flexural waves rarely radiate any acoustic power, that is, the radiation efficiency for low frequencies than critical frequency is negligible.

The phenomena of impact excited plate with attached layer are shown in Fig. 10. In Fig.10, the magnitude decreases much in comparison with the case of bare steel plate. The time interval between the first and second peaks of the acceleration and sound pressure are connected

with the flexural wave speed.

The peak sound pressure levels calculated from Eq.(12) agree well with the measured values for various layer thicknesses, as shown in the TABLE.

Table. Measured and calculated values of the maximum peak sound pressure levels for various layer thickness. 2mm-thick. bare steel plate, H= 0.052m 1.504 cm-steel ball, a=14 cm.

Layer thick. (rubber)	Measured / Calculated $\psi = 0^\circ$, R = 10 cm	
0.	125.8 dB	125.5 dB
1.7 mm	123.6	122.9
2.7 mm	122.9	122.1
3.5 mm	122.7	121.6

In Eqs.(12) and (13), we can find the important parameter in impact transient sound generation. It is apparent that the radiated sound pressure is directly proportional to the impact force and inversely proportional to the mass

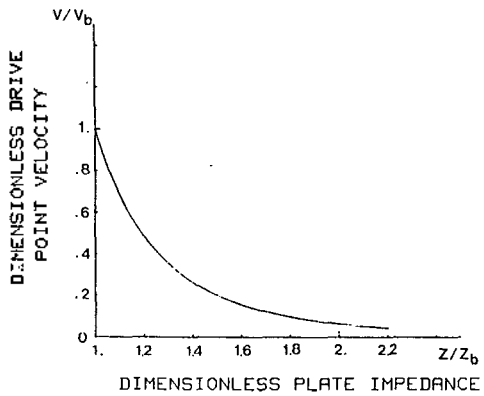

Fig.14 Dimensionless drive point velocity of a plate as a function of plate impedance. Subscript b denotes the bare steel plate and no subscript denotes the plate with viscoelastic layer.

of the plate. Also the impedance values is directly related to the drive point velocity of the plate. From Eq.(14), the drive point velocity of the plate with viscoelastic layer can be approximated as

$$\frac{V}{V_b} = \left(\frac{Z_b}{Z}\right) \tag{15}$$

where subscript b denotes the bare steel plate and V_b is given as $F_w/Z_b(1+1.1\lambda)$. The Eq. (15) has been plotted for various impedance of the plate in Fig.14.

V. CONCLUSIONS

Axisymmetric transient sound radiation from the clamped circular plate with or without attached layer has been obtained. The results of the theoretical analysis agree with those of experiments on the sound radiation by impact force. The waveforms of sound pressure are evaluated by Rayleigh integral and Mindlin's plate theory including rotatory inertia and shear deformation. This analytical results can be applicable to multilayered plate.

We find a method to reduce the impact noise and vibration from the analytical and experimental results. Then we suggest a method reducing the noise in according to the state whether the first peak by rigid body radiation or the ringing radiation by the free damped vibration dominates in impact noise. In both cases, the decrease in the magnitude of impact force results in the reduction of the peak level of the radiated sound pressure and vibration. When the magnitude of the first peak pressure is higher than that of the free vibration sound, it is important to decrease the impact force and to increase the duration of the impact. In the opposite case, we have to increase the damping

in order to reduce the ringing noise. However, in the case of the high damped plate, the first peak level may be a dominated source of sound on the axis of impact point. In order to satisfy this both cases, the plate with viscoelastic layer is useful.

Although the results for the velocity response and the sound radiation on the two layered plate are given in this paper, the present evaluation can be extended to the problems of multi-layered viscoelastic plate.

REFERENCES

1. A. Akay, "A review of impact noise," J. Acoust. Soc. Am. 64,977-987 (1978).
2. M. Strasberg, "Radiation from a diaphragm struck periodically by a light mass," J. Acoust. Soc. Am. 20,683-690 (1984).
3. M. Lax, "The effect of radiation on the vibrations of a circular diaphragm," J. Acoust. Soc. Am. 16,5-13 (1944).
4. A. Akay and M. Latcha, "Sound radiation from an impact-excited clamped circular plate in an infinite baffle," J. Acoust. Soc. Am. 74,640-648 (1983).
5. A. Akay, M. Tokunaga, and M. Latcha, "The theoretical analysis of transient sound radiation from a clamped circular plate," J. Appl. Mech. Trans. ASME 51,41-47 (1984).
6. T. Takahagi and M. Nakai, "The approximation of pressure waveforms of impact sound radiation from clamped circular plate of various thickness," J. Acoust. Soc. Am. 78,2049-2057 (1985).
7. S. Venkatesan and V.X. Kunukkasseril, "Free vibration of layered circular plate," J. Sound Vib. 60(4), 511-534 (1978).
8. Krzysztof Poltorak and Kosuke Nagays, "A method for solving free viration problems of three-layered plates with arbitrary shape," J. Acoust. Soc. Am. 78(6), 2042-2048 (1985).
9. J.W. Phillips and H.H. Calvit, "Impact of a regid sphere on a viscoelastic plate," J. Appl. Mech. Trans. ASME, 873-878 (1967).
10. W. Goldsmith, *IMPACT*, Edward Anold LTD, London, 1960, Chap.IV.
11. Lord Rayleigh, *Theory of Sound*, Vol II (Dover, New York, 1945), Sec.278.
12. P.M. Morse and K.U. Ingard, *Theoretical, Acoustics*, McGraw Hill, New York, 1968, Chap.7.